Neurobiology of Disease

The Role of Cysteine String Protein α Phosphorylation at Serine 10 and 34 by Protein Kinase Cγ for Presynaptic Maintenance

Toshihiko Shirafuji,[1] **Takehiko Ueyama,**[3] **Naoko Adachi,**[3] **Ken-Ichi Yoshino,**[3] **Yusuke Sotomaru,**[2] **Junsuke Uwada,**[4] **Azumi Kaneoka,**[1] **Taro Ueda,**[1] **Shigeru Tanaka,**[1] **Izumi Hide,**[1] **Naoaki Saito,**[3] **and Norio Sakai**[1]

[1]Department of Molecular and Pharmacological Neuroscience, Graduate School of Biomedical Sciences, and [2]Natural Science Center for Basic Research and Development, Hiroshima University, Hiroshima 734-8551, Japan, [3]Laboratory of Molecular Pharmacology, Biosignal Research Center, Kobe University, Kobe 657-8501, Japan, and [4]Division of Cellular Signal Transduction, Department of Biochemistry, Asahikawa Medical University, Asahikawa 078-8510, Japan

Protein kinase Cγ (PKCγ) knock-out (KO) animals exhibit symptoms of Parkinson's disease (PD), including dopaminergic neuronal loss in the substantia nigra. However, the PKCγ substrates responsible for the survival of dopaminergic neurons *in vivo* have not yet been elucidated. Previously, we found 10 potent substrates in the striatum of PKCγ-KO mice. Here, we focused on cysteine string protein α (CSPα), a protein from the heat shock protein (HSP) 40 cochaperone families localized on synaptic vesicles. We found that in cultured cells, PKCγ phosphorylates CSPα at serine (Ser) 10 and Ser34. Additionally, apoptosis was found to have been enhanced by the overexpression of a phosphorylation-null mutant of CSPα, CSPα(S10A/S34A). Compared with wild-type (WT) CSPα, the CSPα(S10A/S34A) mutant had a weaker interaction with HSP70. However, in sharp contrast, a phosphomimetic CSPα(S10D/S34D) mutant, compared with WT CSPα, had a stronger interaction with HSP70. In addition, total levels of synaptosomal-associated protein (SNAP) 25, a main downstream target of the HSC70/HSP70 chaperone complex, were found to have decreased by the CSPα(S10A/S34A) mutant through increased ubiquitination of SNAP25 in PC12 cells. In the striatum of 2-year-old male PKCγ-KO mice, decreased phosphorylation levels of CSPα and decreased SNAP25 protein levels were observed. These findings indicate the phosphorylation of CSPα by PKCγ may protect the presynaptic terminal from neurodegeneration. The PKCγ–CSPα–HSC70/HSP70 –SNAP25 axis, because of its role in protecting the presynaptic terminal, may provide a new therapeutic target for the treatment of PD.

Key words: chaperone; cysteine string protein α; phosphorylation; presynapse; protein kinase C

Significance Statement

Cysteine string protein α (CSPα) is a protein belonging to the heat shock protein (HSP) 40 cochaperone families localized on synaptic vesicles, which maintain the presynaptic terminal. However, the function of CSPα phosphorylation by protein kinase C (PKC) for neuronal cell survival remains unclear. The experiments presented here demonstrate that PKCγ phosphorylates CSPα at serine (Ser) 10 and Ser34. CSPα phosphorylation at Ser10 and Ser34 by PKCγ protects the presynaptic terminal by promoting HSP70 chaperone activity. This report suggests that CSPα phosphorylation, because of its role in modulating HSP70 chaperone activity, may be a target for the treatment of neurodegeneration.

Introduction

Protein kinase C (PKC) is an important serine/threonine (Ser/Thr) kinase implicated in various cellular functions, including the regulation of cell survival (Ruvolo et al., 1998; Whelan and Parker, 1998), and in Ca^{2+}-triggered exocytosis (Iwasaki et al., 2000; Barclay et al., 2003; Shirafuji et al., 2014). The PKC family consists of at least 10 subtypes and is divided into the following three subfamilies: conventional PKC (cPKC), novel PKC, and

atypical PKC (Nishizuka, 1992). Among PKCs, only cPKCs (including PKCγ, which is a neuron-specific PKC isoform; Saito and Shirai, 2002) are activated by Ca^{2+} because they contain a C2 domain that specifically binds to Ca^{2+} and phosphatidylserine (PS; Murray and Honig, 2002). PKCγ knock-out (KO) animal models exhibit parkinsonian symptoms in an age-dependent manner. These symptom include dopaminergic neuronal cell loss in the substantia nigra (SN; Payne et al., 2000). Further, increased ubiquitination levels in dopaminergic and serotonergic neurons have also been reported in PKCγ-KO rats at 18 months of age (Al-Kushi, 2007). Although antiapoptotic/prosurvival functions of cPKC have been demonstrated (Ruvolo et al., 1998; Whelan and Parker, 1998), little is known about cPKC's function related to chaperone regulation in the presynaptic terminal of neurons.

Using the shotgun phosphoproteome, we have previously identified 10 candidates for PKCγ substrates in the nigro-striatum system (Shirafuji et al., 2014). One of these candidates is cysteine (Cys) string protein α (CSPα), which we focused on in the present study. CSPα is a member of the HSP40/DNAJ family of cochaperones, characterized by the presence of the J domain (Ohtsuka, 1993), named after the *Escherichia coli* protein DNAJ (Yochem et al., 1978). The J domain is responsible for interactions with HSC70/HSP70 through the histidine, proline, and aspartic (HPD) motif and helix II (Szyperski et al., 1994; Hill et al., 1995). HSP40/DNAJ binding regulates the ATPase activity of HSC70/HSP70, which helps prevent denatured proteins from aggregating (Braun et al., 1996).

The HSP40/DNAJ family consists of ≥50 members (Qiu et al., 2006). These have been classified into three subtypes: HSP40 type 1, 2, and 3 (also referred to as DNAJ A–C; Cheetham and Caplan, 1998). The members of this family differ from each other by subcellular location and tissue distribution. CSPα belongs to the HSP40 type-3 (DNAJC) subtype and is highly expressed in all neurons, where it is localized on synaptic vesicle membranes in the presynaptic terminal (Chamberlain and Burgoyne, 2000). In neurodegenerative diseases, presynaptic terminals degenerate before the loss of neuronal somata, according to reports (Wishart et al., 2006). As deletion of CSPα also causes presynaptic degeneration in flies (Zinsmaier et al., 1994), worms (Kashyap et al., 2014), and mice (Fernández-Chacón et al., 2004), CSPα clearly performs a universal neuroprotective function (Burgoyne and Morgan, 2015), especially at the presynaptic terminal. To date, although there have been several studies on CSPα phosphorylation associated with exocytosis (Evans et al., 2001, 2006), the involvement of CSPα phosphorylation in the regulation of HSC70/HSP70 chaperone activity and the protection of the presynaptic terminal has not been reported.

In the present study, we have found that CSPα is phosphorylated by PKCγ at Ser10 and Ser34. CSPα phosphorylation by PKCγ may promote its interaction with HSC70/HSP70 and chaperone activity for synaptosomal-associated protein (SNAP) 25 in the presynaptic terminal of dopaminergic neurons.

Materials and Methods

Antibodies. The anti-green fluorescent protein (GFP) antibody (Ab) was generated in house (Shirafuji et al., 2014). The following Abs were purchased: anti-FLAG (#P2983), anti-β-tubulin (T-4026), and anti-tyrosine hydroxylase (TH; T-1299) from Sigma-Aldrich; anti-glutathione S-transferase (GST; #sc-33613), anti-PKCγ (#sc-211), and anti-ubiquitin (sc-8017) from Santa Cruz Biotechnology; anti-pSer PKC motif (#2261), anti-pThr (#9381), anti-cleaved caspase-3 (#9661), and anti-Myc (#2276) from Cell Signaling Technology; anti-CSPα (ab90499) and anti-SNAP25 (ab41455) from Abcam; anti-CSPα (AB1576) and anti-SNAP25 (MAB331) from Millipore; and HRP-conjugated anti-rabbit and anti-mouse secondary Abs

from Jackson ImmunoResearch. The anti-TH (T-1299), anti-ubiquitin (sc-8017), anti-pSer PKC motif (#2261), anti-SNAP25 (ab41455), anti-SNAP25 (MAB331), anti-CSPα (ab90499), and anti-cleaved caspase-3 (#9661) Abs were verified by our laboratory (Shirafuji et al., 2017). The vendor provided a datasheet for anti-PKCγ (#sc-211), which showed that this Ab has no cross-reactivity to other PKCs. Anti-CSPα (AB1576) has been verified previously (Kohan et al., 1995).

Animals. A PKCγ-Cre knock-in (KI) mouse was provided by ZF Chen (Ding et al., 2005). After the sixth backcross, male homozygous littermates obtained by crossing heterozygous PKCγ-Cre-KI mice were used as PKCγ KOs in the present study, along with wild-type (WT) mice. All animal studies were approved by the Hiroshima University Institutional Animal Care and Use Committee and conducted according to the Hiroshima University Animal Experimentation Regulations.

Cell culture. COS7 cells were cultured in DMEM (Nacalai Tesque), supplemented with 10% fetal bovine serum, penicillin (100 U/ml), and streptomycin (100 μg/ml). PC12 cells were cultured in DMEM containing 5% fetal bovine serum and 10% horse serum. All cells were cultured at 37°C in a humidified atmosphere containing 5% carbon dioxide.

Construction of plasmids. WT human PKCγ was cloned into pcDNA3.1 (Life Technologies), and the subdomains of PKCγ were cloned into pcDNA3.1 with GFP, as described previously (Shirafuji et al., 2014). Human influenza hemagglutinin (HA)-tagged ubiquitin cDNA was a gift from Dr. Yamashita (Nagano et al., 2003). Human CSPα, SNAP25, and small glutamine-rich tetratricopeptide repeat-containing protein 1 (SGT1) were provided by the RIKEN Bio Resource Center through the National Bio Resource Project of the Ministry of Education, Culture, Sports, Science, and Technology in Ibaraki, Japan (Ota et al., 2004). For construction of the plasmid encoding a full-length CSPα fused to GST, full-length CSPα with an EcoRI/XhoI site was amplified by PCR and cloned into the pGEX-6P1 vector (GE Healthcare). For the construction of plasmids encoding CSPα, HSP40, HSP70, SGT1, and SNAP25 fused with 3xFLAG at the N terminal, each protein with an EcoRI/BamHI site, amplified via PCR, was cloned into a 3xpFLAG-CMV10 vector (Sigma-Aldrich). For the construction of a plasmid encoding HSC70 fused with 3xFLAG at the N terminal, HSC70 with a BglII/BamHI site, amplified via PCR, was cloned into a 3xpFLAG-CMV10 vector. For the construction of a plasmid encoding full-length CSPα fused with enhanced GFP (EGFP) at the N terminal, CSPα with a XhoI/EcoRI site, produced by PCR, was cloned into a pEGFP-C1 vector (Clontech). For the construction of a plasmid encoding HSP70 fused with Myc tag at the C terminal, HSP70 with an EcoRI/XhoI site, amplified via PCR, was cloned into a pcDNA3.1 Myc vector (Thermo Fisher Scientific). Substitutions of Ser for alanine (Ala), glutamate (Glu), or aspartate (Asp) at the identified phosphorylation sites (Ser10Ala, Ser34Ala, Ser81Ala, Ser10Ala/Ser34Ala, Ser10Glu/Ser34Glu, and Ser10Asp/Ser34Asp) were introduced with a QuikChange Multisite-Directed Mutagenesis Kit (Agilent Technologies). All cDNAs were verified by sequencing.

RNA interference and short hairpin RNA-resistant CSPα plasmid construction. Double-stranded oligonucleotides were cloned into a short hairpin RNA (shRNA) expression vector, pSuper (puro; Oligoengine). The target sequences for the shRNA rat CSPα were GCTACTGCTGCT GCTGTTTAT (sh356; cording nucleotides 356–376) and GCTGTTTT ATGCTGTTGCTTTA (sh368; cording nucleotides 368–388). Because the target sequence for the rat CSPα knockdown (KD; sh356 and sh368) was located in the coding region of CSPα, sh356-resistant and sh368-resistant human CSPα in the 3xpFLAG-CMV10 vector was generated by introducing seven-base and eight-base silent changes for sh368 and sh356, respectively, within the targeting sequence (5′ GtTAtTGtTGCT GtTGc ′3 356–372), with a QuikChange Multisite-Directed Mutagenesis Kit. All cDNAs were verified by sequencing.

Protein expression. Protein expression was performed, as described previously (Ueyama et al., 2007). In brief, BL21 pLys *E. coli* and Sf9 cells were transformed using expression plasmids. *E. coli* and Sf9 cells were harvested and lysed. For the purification of recombinant proteins, GST fusion proteins were purified with glutathione-Sepharose 4B resin (GE Healthcare Biosciences).

In vitro PKC phosphorylation assay. An *in vitro* PKC phosphorylation assay was performed, as described previously (Shirafuji et al., 2014). In

brief, purified GST-tagged CSPα was incubated with 200 ng of GST-tagged PKCγ, or GST, and the following buffers: 20 mM Tris, pH 7.4, 0.5 mM calcium chloride, 10 μM adenosine triphosphate (ATP), 8 μg/ml PS, and 0.8 μg/ml (±)-1,2-didecanoylglycerol (DO), in a 50 μl final volume for 30 min. Immunoblotting for anti-pSer PKC Ab and anti-GST Ab was performed.

PKC phosphorylation assay in cultured cells. A PKC phosphorylation assay in cultured cells was performed, as described previously (Shirafuji et al., 2014), albeit with slight modifications. In brief, COS7 cells were transfected with WT CSPα in 3xpFLAG-CMV10 with a NEPA21 electroporator (Nepa Gene). After 12-O-tetradecanoylphorbol 13-acetate (TPA) stimulation, with or without PKC inhibitors GF109203X (GFX), a pan PKC inhibitor, and Gö6976, a classical PKC inhibitor, for 30 min in HEPES buffer at 37°C, cells were collected and resuspended in homogenization buffer containing 150 mM sodium chloride (NaCl), 10 mM ethylene glycol tetraacetic acid, 2 mM ethylenediamine tetraacetic acid, 10 mM HEPES, pH 7.4, 1 mM phenylmethylsulfonyl fluoride, 20 μg/ml leupeptin, and a phosphatase inhibitor mixture. The precipitated proteins by anti-FLAG Ab were separated via SDS-PAGE. The phosphorylated proteins were visualized with phospho-Abs. For the calculation of relative phosphorylation levels, the densitometries of the immunoblots of the phospho-Abs were normalized to the total protein levels in each experiment; the averages of the relative levels of phosphorylation in >3 independent experiments have been presented. Phosphorylation levels of the prestimulations were defined as 1.00.

Sample preparation and Western blot analysis. Mouse brains and cells were homogenized and the concentrations of proteins were measured using a bicinchoninic acid protein assay kit (Thermo Fisher Scientific). SDS-PAGE and immunoblot analyses were performed, as described previously (Shirafuji et al., 2014).

Coimmunoprecipitation. The cells and mouse striatum samples were collected and resuspended in homogenization buffer containing 150 mM NaCl, 10 mM ethylene glycoltetraaceticacid, 2 mM ethylenediamine tetraacetic acid, 10 mM HEPES, pH 7.4, 1 mM phenylmethylsulfonyl fluoride, 20 μg/ml leupeptin, and a phosphatase-inhibitor mixture. Proteins precipitated by anti-FLAG, Myc, CSPα, and SNAP25 Abs were separated by SDS-PAGE and immunoblotted by appropriate Abs.

In-gel digestion. After destaining, each sliced gel was incubated with 10 mM dithiothreitol in 25 mM ammonium bicarbonate for 60 min at 50°C for reduction, and then with 0.1 M iodoacetamide in 50 mM ammonium bicarbonate for 45 min at room temperature for alkylation. For protein digestion, 200 ng of porcine trypsin or bovine chymotrypsin [mass spectrometry (MS) grade; Thermo Fisher Scientific] in 25 mM ammonium bicarbonate was added to each sliced gel in a tube, and the endopeptidase-solution-absorbed gel was then incubated for 2 h at 37°C (trypsin) or 25°C (chymotrypsin). Endopeptidase digestion was halted by addition of 5% formic acid. After incubation for 15 min at room temperature, 5% formic acid/50% acetonitrile was added to each tube and incubated for 15 min at room temperature for extraction of peptide fragments from the gels. The supernatant was transferred into another tube made of TPX (IEDA Trading). Then, 100% acetonitrile was added to each sliced gel in a tube and incubated for 15 min at room temperature. The supernatant was collected into the same TPX tube. The collected extract was dried down in a vacuum centrifuge.

Liquid chromatography/MS/MS. Liquid chromatography/MS/MS (LC/MS/MS) was performed on an LTQ-Orbitrap Discovery linear ion trap–orbitrap tandem mass spectrometer (Thermo Fisher Scientific), which was connected to a Dionex UltiMate 3000 pump and a HTC-PAL autosampler (CTC Analytics). The mobile phases consisted of 0.1% formic acid in water (solvent A) and 0.1% formic acid in acetonitrile (solvent B).

Dried peptide fragments dissolved in 20 μl of 0.1% trifluoroacetic acid were applied to the LC/MS/MS system. The peptides were fractionated on an L-column Micro C-18 (150 mm length × 100 μm inner diameter; particle size, 3 μm; Chemicals Evaluation and Research Institute) with a linear gradient of 3– 43% solvent B for 40 min at a flow rate of 500 nl/min. The column eluent was sprayed directly into the ion source of the mass spectrometer, using a spray tip (Fortis tip, AMR) with a spray voltage of 1.8 kV. The "lock mass" function was used to obtain high mass accuracy

during the fractionation. The mass spectra were measured in a range of 300–2000 *m/z* ratio. In each mass spectrum of eluents, the top seven high-intensity precursor ions were selected automatically for subsequent product ion analysis by a data-dependent scan mode with a dynamic exclusion option.

The LC/MS/MS data were interpreted using a Mascot MS/MS ions search (Matrix Science). Peptides and proteins were identified from the Swiss-Prot database, with a peptide mass tolerance of 4 ppm and a fragment mass tolerance of 0.8 Da. Carbamidomethylation at Cys sites and phosphorylation at Ser/Thr sites were allowed as variable modifications.

Statistical analysis. The data are presented as mean ± SEM and were analyzed with two-sided, unpaired *t* tests and one-way ANOVA with a *post hoc* Dunnett's test, Games–Howell's test, or Tukey's test. Statistical analyses were performed with the Statview 5.0J software package (SAS Institute). *P* values of ≤5% were considered statistically significant.

Results
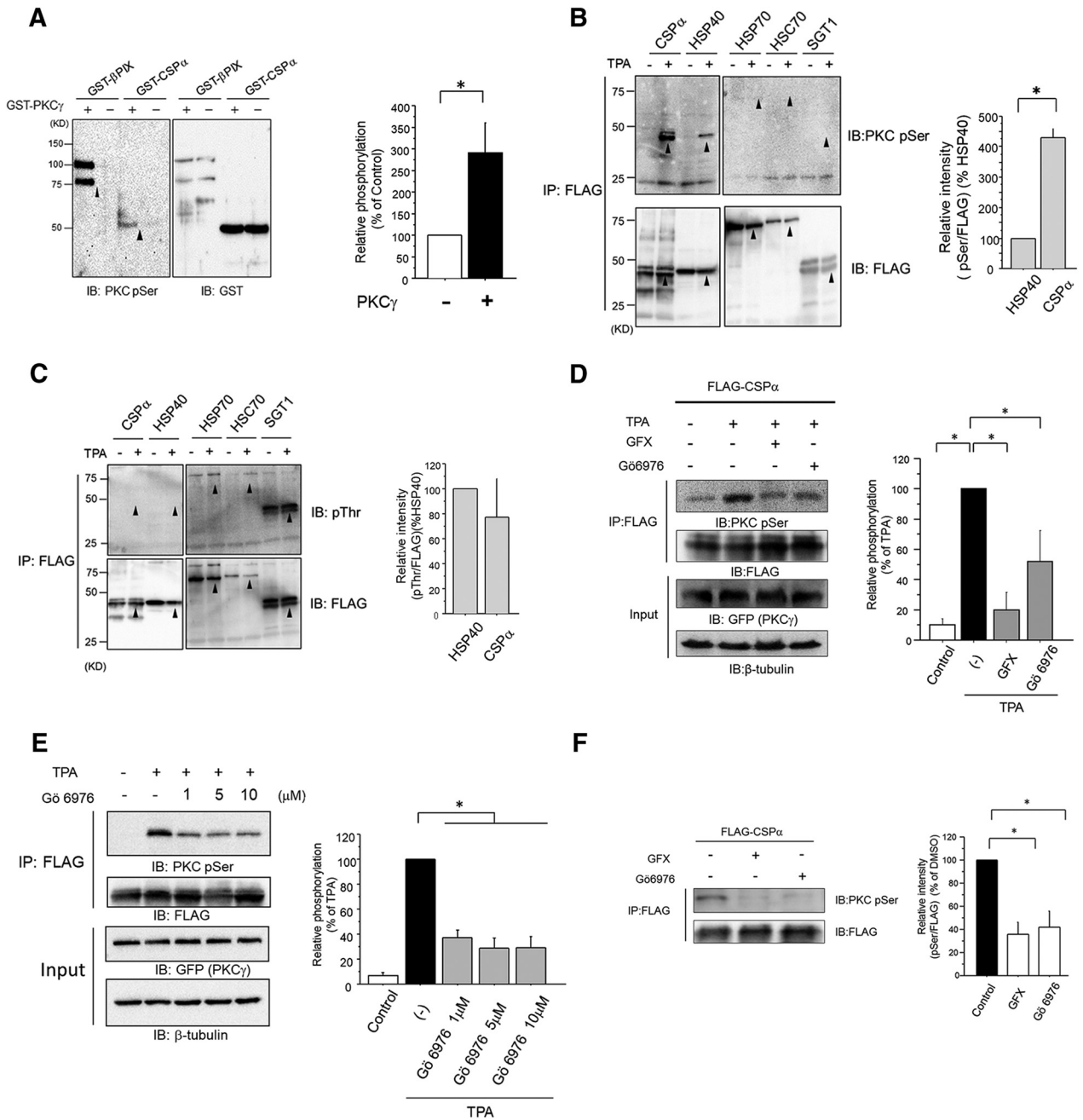## CSPα is phosphorylated by PKCγ *in vitro* and in cultured cells
Previously, through phosphoproteome analysis, we identified the CSPα phosphorylation at Ser10 by PKCγ, (Shirafuji et al., 2014). To verify whether CSPα is phosphorylated by PKCγ, we performed phosphorylation experiments *in vitro* and in cultured cells. In *in vitro* experiments, GST-tagged CSPα and GST-tagged PKCγ, or GST, were incubated with PS/DO/Ca^{2+}, which is the PKC stimulator. Enhanced phosphorylation of FLAG-tagged CSP extracted from COS7 cells, transfected with FLAG-tagged CSP and with GFP-tagged PKC, was observed with an anti-Ser PKC motifAb, but not with an anti-pThr Ab, after treatment with 1 M TPA, which is a PKC stimulator (Fig. 1B,C). Furthermore, TPA-induced phosphorylation of CSPα was found to have reduced by Gö6976, which is a cPKC inhibitor, and GFX, which is a pan-PKC inhibitor at a cellular level (Fig. 1D). No significant enhancement of the effect of Gö6976 was observed when the concentration was increased above 1 μM, suggesting that PKCs other than cPKC may also phosphorylate CSPα upon TPA stimulation in COS7 cells (Fig. 1E).

Decreased phosphorylation of FLAG-tagged CSPα, extracted from PC12 cells transfected with FLAG-tagged CSPα, was observed with an anti-Ser PKC motif Ab after treatment with 1 μM PKC inhibitors Gö6976 and GFX (Fig. 1F). In summary, although other serine kinases, such as protein kinase A (PKA; Evans et al., 2001), may phosphorylate CSPα to a lesser extent, CSPα is phosphorylated mainly by PKCγ *in vitro* and in cultured cells.

cPKC phosphorylates CSPα at Ser10 and Ser34 in cultured cells
Because CSPα contains several predicted PKC phosphorylation sites, such as Ser10, Ser34, and Ser81 (Fig. 2A), we investigated whether CSPα was phosphorylated at Ser10, Ser34, and Ser81 within cells by using CSPα(S10A), CSPα(S34A), and CSPα(S81A) mutants, which are phosphorylation-null mutants. CSPα(S10A) and CSPα(S34A), but not CSPα(S81A), were less phosphorylated in TPA-treated COS7 cells compared with WT CSPα (Fig. 2B). Further, CSPα(S10A), CSPα(S34A), and CSPα(S10A/S34A) mutants were less phosphorylated in PC12 cells, compared with WT CSPα (Fig. 2C). To demonstrate the phosphorylation of CSPα at Ser10 and Ser34, we performed phosphorylation assays *in vitro* and in cultured cells, followed by MS. We identified phosphorylation at Ser10 in the trypsin digest of GST-tagged CSPα (Fig. 2D) and at Ser34 in the chymotrypsin digest of FLAG-tagged CSPα (Fig. 2E). These findings indicate that CSPα residues Ser10 and Ser34 are phosphorylated by cPKC.

Figure 1. CSPα is phosphorylated by PKCγ *in vitro*. ***A***, *In vitro* phosphorylation of CSPα. GST-tagged CSPα proteins were incubated with or without recombinant PKCγ in the presence of PKC activator (PS/DO/Ca^{2+}) and ATP for 30 min. The phosphorylated proteins were detected by immunoblot for anti-pSer PKC motif Ab, and protein expression was determined by immunoblot with an anti-GST Ab. βPIX is a positive control. The arrowheads on the left panel indicate the bands of immunoblot for anti-pSer PKC motif Ab, and those on the right indicate the total proteins immunoblotted by anti-GST Ab. The phosphorylation levels of GST-tagged CSPα with PKCγ were normalized to those without PKCγ phosphorylation, which were set at 100%, as shown in the bar graph ($n = 3$, *$p < 0.05$, unpaired t test). ***B***, ***C***, COS7 cells expressing FLAG-tagged CSPα, HSP40, HSP70, HSC70, and SGT1 were stimulated with 1 μM TPA for 30 min. Phosphorylated proteins were detected by immunoblotting for the anti-pSer PKC motif Ab (***B***) and anti-pThr Ab (***C***), and protein expression was determined by immunoblots with an anti-FLAG Ab. Arrowheads on the top panels indicate the bands for the anti-pSer PKC motif and anti-pThr Abs, or the assumed positions for the anti-pSer PKC motif and anti-pThr Abs, if any. The arrowheads on the bottom panels indicate the total proteins immunoblotted by the anti-FLAG Ab. The phosphorylation levels of CSPα with anti-pSer PKC motif Ab and anti-pThr Abs were normalized to the HSP40 phosphorylation signal, which was set to 100%, as shown in the graph ($n = 3$ for each; *$p < 0.05$, unpaired t test). The results are expressed as mean ± SEM. ***D***, Cellular phosphorylation of CSPα. COS7 cells expressing FLAG-tagged CSPα and GFP-tagged PKCγ were stimulated with 1 μM TPA in the presence or absence of 1 μM GFX, or Gö6976 for 30 min. FLAG-tagged CSPα proteins were purified with anti-FLAG agarose resin. Phosphorylated proteins were detected by an immunoblot analysis with an anti-pSer PKC motif Ab. Protein expression was determined by immunoblot with an anti-FLAG Ab. The right bar graph represents the quantification of phosphorylation levels of FLAG-tagged CSPα normalized to that of 1 μm TPA stimulation, which was set to 100% ($n = 6$; *$p < 0.05$, 1-way ANOVA with *post hoc* Tukey's test). The results are expressed as mean ± SEM. ***E***, COS7 cells expressing FLAG-tagged CSPα and GFP-tagged PKCγ were stimulated with 1 μM TPA in the presence of 1, 5, and 10 μM Gö6976 for 30 min. The phosphorylation levels of FLAG-tagged CSPα were normalized to that of 1 μM TPA stimulation, which was set to 100%, as shown in right bar graph ($n = 6$; *$p < 0.05$, 1-way ANOVA with *post hoc* Tukey's test). The results are expressed as mean ± SEM. ***F***, PC12 cells expressing FLAG-tagged CSPα were incubated for 72 h in the absence or presence of 1 μM GFX and Gö6976. FLAG-tagged CSPα proteins were purified with anti-FLAG agarose resin. Phosphorylated proteins were detected by immunoblot for the anti-pSer PKC motif Ab, and protein expression was determined by immunoblots with an anti-FLAG Ab. The phosphorylation levels of FLAG-tagged CSPα were normalized to that of the control, which was set to 100%, as shown in the right bar graph ($n = 4$; *$p < 0.05$, 1-way ANOVA with *post hoc* Tukey's test). The results are expressed as mean ± SEM.

A

B

C

D

E
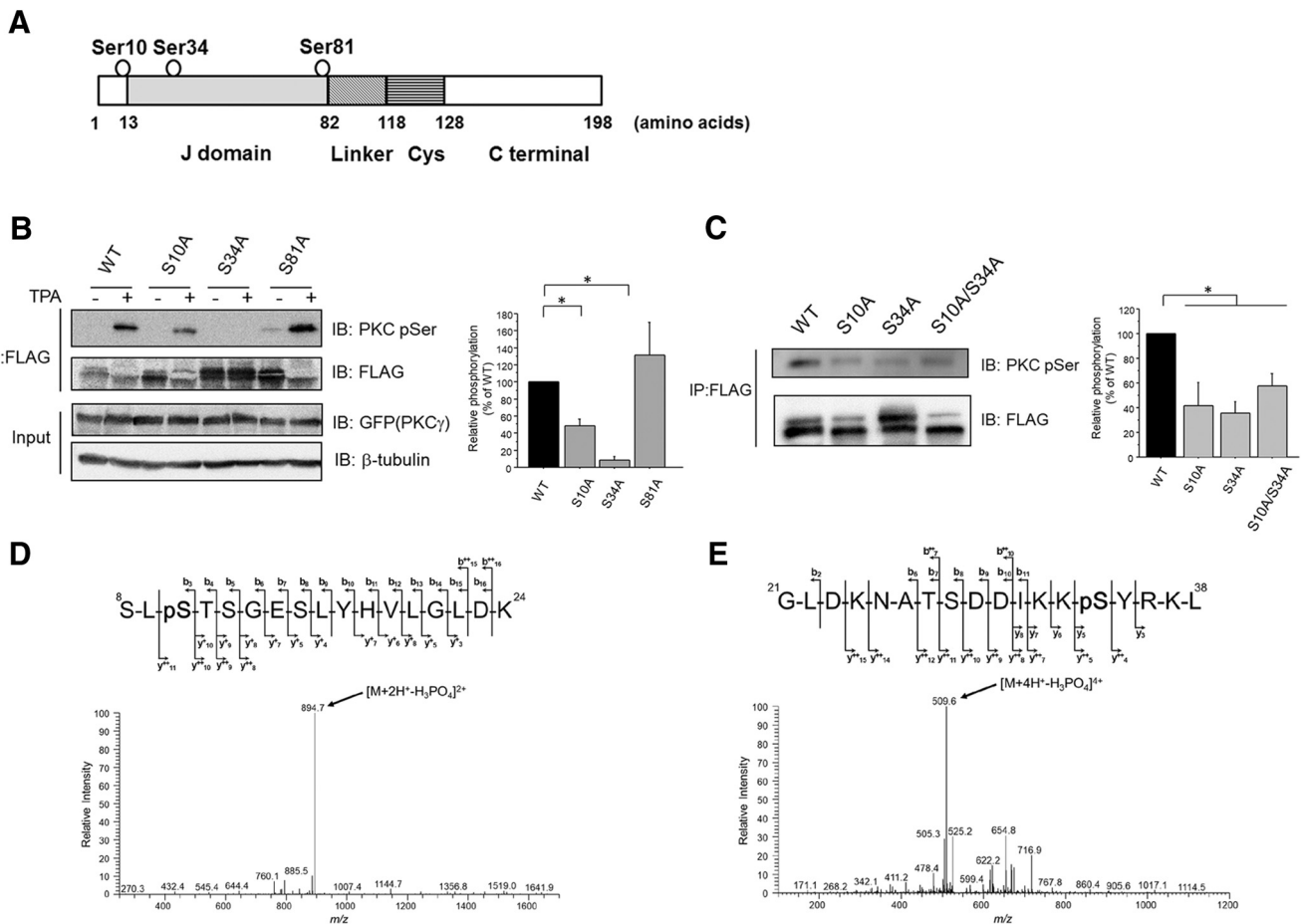
Figure 2. cPKC mediates the phosphorylation of CSPα at Ser10 and Ser34 in cultured cells. ***A***, Schematic illustrations of the CSPα. The predicted phosphorylation sites are circled. Cys, Cysteine string domain. ***B***, COS7 cells transfected with FLAG-tagged CSPα (WT and Ser/Ala mutants) and GFP-tagged PKCγ were stimulated with 1 μM TPA for 30 min. FLAG-tagged CSPα was precipitated and separated by SDS-PAGE. The phosphorylation levels of the FLAG-tagged CSPα proteins determined with an anti-pSer PKC Ab were normalized to the protein levels of the CSPα (WT and Ser/Ala mutants) determined by immunoblots with an anti-FLAG Ab. The right bar graph shows the relative phosphorylation levels normalized to the WT CSPα levels, which were set as 100% ($n = 6$, $*p < 0.05$ vs WT, 1-way ANOVA with *post hoc* Games–Howell test). ***C***, PC12 cells transfected with FLAG-tagged CSPα (WT and Ser/Ala mutants) were incubated for 72 h. The phosphorylation levels of the FLAG-tagged CSPα proteins determined with an anti-pSer PKC Ab were normalized to the protein levels of the CSPα (WT and Ser/Ala mutants), determined by immunoblots with an anti-FLAG Ab. The right graph shows the relative phosphorylation levels normalized to the WT CSPα levels, which were set as 100% ($n = 6$, $*p < 0.05$ vs WT, 1-way ANOVA with *post hoc* Dunnett's test). ***D***, HPLC/MS/MS spectrum of phosphopeptide representing 8 –24 residues of CSPα after PKCγ assay. Product ion spectrum of the doubly charged peptide at m/z ratio 943.4528 was acquired on a linear ion trap mass spectrometer. The predominant product ion at m/z ratio 894.7 generated by neutral loss of 98.0 Da (H_3PO_4) is clearly visible, featuring a product ion spectrum of a phosphoserine/phosphothreonine-containing peptide. Sequence-revealing product ions appeared at relatively weak intensity; however, they were sufficient to distinguish the exact site (S10) of phosphorylation among five potential sites (S8, S10, T11, S12, and S15). ***E***, HPLC/MS/MS spectrum of phosphopeptide representing 21–38 residues of CSPα after PKC assay. Product ion spectrum of the quadruply charged peptide m/z ratio 533.7739 was acquired on a linear ion trap mass spectrometer. The predominant product ion at m/z ratio 509.6 generated by neutral loss of 98.0 Da (H3PO4) is clearly visible, featuring a product ion spectrum of a phosphoserine/phosphothreonine-containing peptide. Sequence-revealing product ions appeared at relatively weak intensity; however, they were sufficient to distinguish the exact site (S34) of phosphorylation among three potential sites (T27, S28, and S34).

CSPα is exclusively phosphorylated by cPKC in the CSPα–HSP70/HSC70–SGT complex at a cellular level

Because CSPα forms a complex with HSC70/HSP70 and SGT (Tobaben et al., 2001), we investigated whether HSC70/HSP70 and SGT were phosphorylated by PKC. It is noted that CSPα can stimulate the ATPase activity of both HSC70 and HSP70 (Chamberlain and Burgoyne, 1997). Moreover, the ATPase domain, which interacts with CSPα J domain, is almost 90% identical between HSC70 and HSP70. It is assumed that HSP70 may be modulated by phosphorylated CSPα in the same manner as HSC70. At a cellular level, HSP70, HSC70, and SGT were not phosphorylated by TPA stimulation, although SGT was ubiquitously phosphorylated at the Thr residue (Fig. 1B, C). These findings suggested that CSPα was exclusively phosphorylated through PKC activation in this complex. Consistent with a previous study using rat brain (Evans and Morgan, 2005), our pre-

vious phosphoproteome analysis revealed extraordinarily high levels of phosphorylation in CSPα (Shirafuji et al., 2014). Almost all protein members of the HSP40/DNAJ family are characterized by Ala residue as the ninth amino acid, upstream of the HPD motif, whereas CSPα is one of the only three HSP40 type-3/ DNAJC family members with Ser residue in the corresponding position. CSPα, which tethers to the synaptic vesicle membrane, could easily be phosphorylated by PKC because PKC phosphorylates substrates bound to membranes (Shirai et al., 1998). Based on these findings, CSPα is supposed to be phosphorylated by PKCγ more strongly than other HSP40/DNAJ families. Therefore, we compared the phosphorylation levels between CSPα (DNAJC5), and HSP40 (DNAJB1). The Ser phosphorylation level of CSPα by PKC was approximately four times higher than that of HSP40 (DNAJB1; Fig. 1B). It must be noted that Thr phosphorylation was not observed in CSPα or HSP40 (DNAJB1;

Fig. 1*C*). These findings suggest that CSPα, compared with other members of the HSP40/DNAJ families, might promote HSC70/HSP70 chaperone activity more strongly through phosphorylation by PKC.

Involvement of cPKC in apoptosis

To study the functional role of PKC and CSPα in the regulation of apoptosis, we examined the levels of cleaved caspase-3 in PC12 cells, a cell line of a dopaminergic neuronal model. PC12 cells express endogenous CSPα and cPKCs, including PKCγ (Shirafuji et al., 2014). The functional role of PKC in the regulation of apoptosis was monitored using Gö6976 and GFX. These PKC inhibitors significantly accelerated apoptosis (Fig. 3*A*). Furthermore, Gö6976 accelerated apoptosis in a dose-dependent manner (Fig. 3*B*). These results suggest that PKC, especially cPKC, plays a crucial role in the apoptosis machinery used within PC12 cells.

CSPα KD suppresses neuronal cell survival

Because CSPα is a cochaperone of HSC70/HSP70, and is reported to protect neurons from degeneration (Zinsmaier et al., 1994; Fernández-Chacón et al., 2004; Kashyap et al., 2014), we investigated the possible involvement of CSPα against apoptosis. KD of CSPα in PC12 cells by shRNA resulted in a significant acceleration of apoptosis. The enhanced apoptosis by CSPα KD in PC12 cells was rescued by WT CSPα and was incomplete (Fig. 3*C*). These data suggest that CSPα plays crucial roles for the survival of PC12 cells.

PKC-mediated phosphorylation of CSPα, at both Ser10 and Ser34, promotes cell survival

To determine the role of PKC-mediated phosphorylation of CSPα in apoptosis, we exogenously introduced WT CSPα and Ser/Ala mutants, including CSPα(S10A), CSPα(S34A), and CSPα(S10A/S34A), into PC12 cells. We found that apoptosis in PC12 cells transfected with FLAG-tagged CSPα(S10A/S34A) significantly increased, compared with PC12 cells transfected with FLAG-tagged WT CSPα (Fig. 3*D*). We also found that apoptosis with CSPα(S10A/S34A) significantly increased in SHSY5Y cells (Fig. 3*E*). Next, we performed this experiment with Ser/Glu or Ser/Asp mutants, including CSPα(S10E/S34E) and CSPα(S10D/S34D) mutants, which are phosphomimetic mutants, in PC12 cells. There were no differences between CSPα(S10E/S34E) or CSPα(S10D/S34D) mutants and WT CSPα (Fig. 3*F*). The fact that phosphomimetic mutants had no additional effects on apoptosis compared with WT CSPα may be explained by the presence of an amount of CSPα protein sufficient for cell survival in PC12 cells, as shown in Fig. 3*D*, in which endogenous CSPα is comparable to exogenously expressed CSPα. Alternatively, the fact may be explained by a high prevalence of phosphorylation in exogenously expressed WT CSPα. This possibility is supported by the following facts: (1) exogenously expressed CSPα was phosphorylated without stimulation in PC12 cells (Fig. 1*F*) and (2) the degree of CSPα phosphorylation was ∼100 times higher than that of other phosphorylated proteins (Shirafuji et al., 2014). Together, our results suggest that PKC-mediated CSPα phosphorylation at both Ser10 and Ser34 positively regulates cell survival.
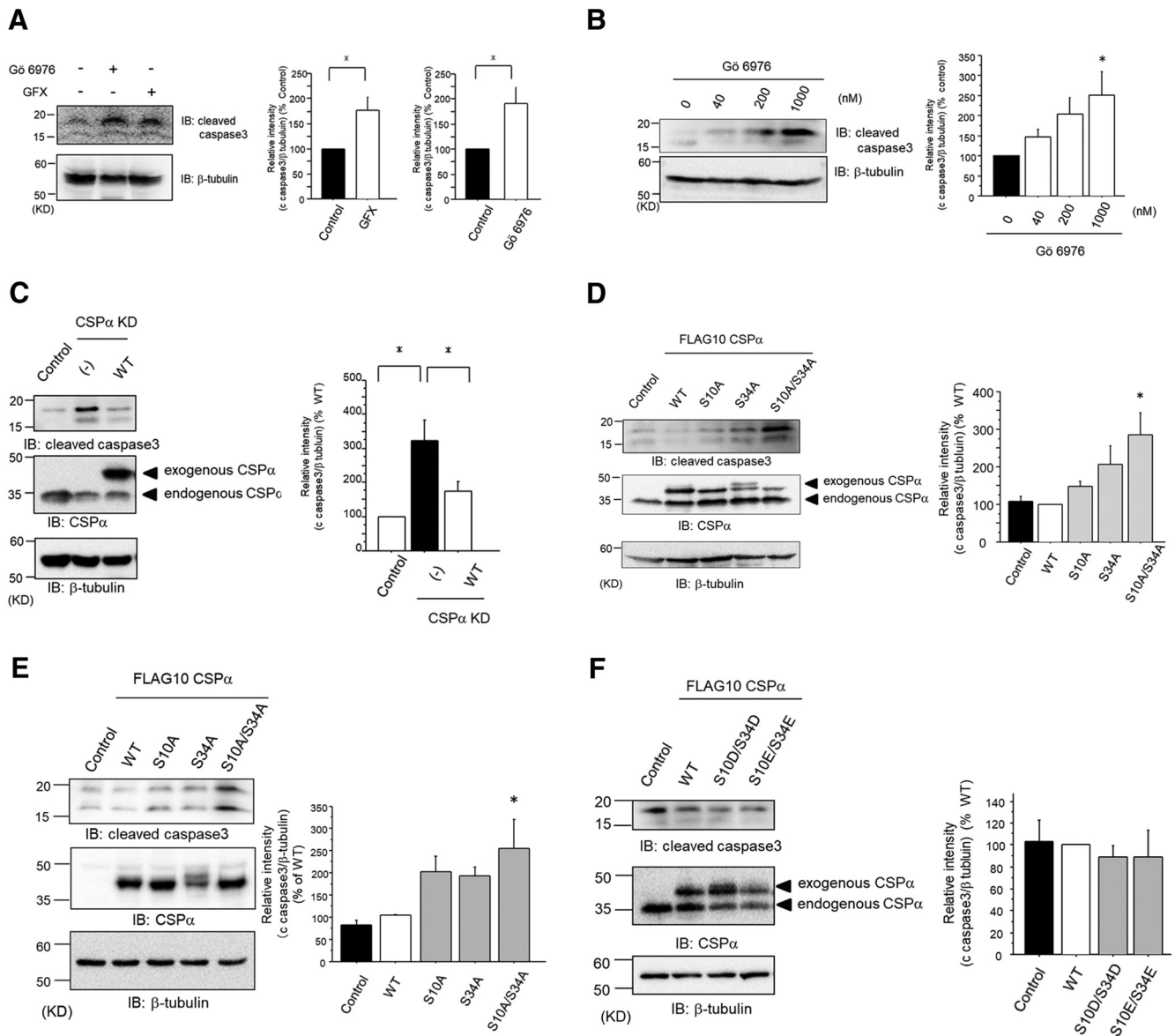
CSPα phosphorylation at Ser10 and Ser34 promotes interaction with HSP70

A previous report (Fang et al., 2013) demonstrated that PKC could potentially promote an interaction between CSPα and HSP70. In the present study, we used PKC stimulator TPA to confirm the enhancing effect of PKC on the interaction between CSPα and HSP70 (Fig. 4*A*,*B*). By contrast, TPA did not promote interaction between HSP40 and HSP70, suggesting that CSPα may be unique among the HSP40 families regulated by PKC (Fig. 4*C*,*D*). Together with targeted phosphorylation on CSPα by PKC among candidates within the CSPα–HSC70/HSP70–SGT complex (Fig. 1*B*,*C*), our results suggested that phosphorylation of residues within CSPα may be crucial for the formation of the CSPα–HSC70/HSP70–SGT complex. Further, to investigate whether Ser10 and/or Ser34 phosphorylation modulates CSPα and HSP70 interaction, we performed a coimmunoprecipitation assay using COS7 cells transfected with Myc-tagged HSP70, along with FLAG-tagged WT CSPα or Ser/Ala mutants. CSPα (S10A/S34A) mutants interacted to a lesser degree with HSP70 than with WT CSPα (Fig. 4*E*). We also investigated the interactions of the CSPα(S10E/S34E) and CSPα(S10D/S34D) mutants with HSP70. The CSPα(S10D/S34D) mutant, compared with WT CSPα or CSPα(S10E/S34E), clearly demonstrated higher interaction with HSP70 (Fig. 4*F*). Because, from a chemical formula point of view, Asp and Glu resemble the phosphorylated Ser and Thr, respectively, CSPα Ser10/34 phosphorylation might be crucial for the increased interaction with HSP70. Thus, CSPα Ser10 and Ser34 two-residue phosphorylation by PKCγ may be important for CSPα–HSC70/HSP70–SGT complex formation, thereby leading to the promotion of HSC70/HSP70 chaperone activity.

CSPα phosphorylation at Ser10 and Ser34 promotes HSC70/HSP70 chaperone activity on SNAP25 in PC12 cells

Previous reports identified many targets for the CSPα–HSC70/HSP70–SGT complex (Leveque et al., 1998; Wu et al., 1999; Magga et al., 2000; Evans and Morgan, 2002; Sakisaka et al., 2002; Boal et al., 2004, 2011; Chandra et al., 2005; Sharma et al., 2011; Shirasaki et al., 2012; Zhang et al., 2012). Among those targets, SNAP25 is thought to be the main one responsible for presynaptic degeneration (Sharma et al., 2011). When the functions of the CSPα–HSC70/HSP70–SGT complex are disturbed, ubiquitination of substrates may increase, suggesting that the ubiquitination level is one of the indicators of the chaperone activity disorder. To examine the function of CSPα phosphorylation on the HSC70/HSP70 chaperone activity on SNAP25, we investigated the degree of ubiquitination on SNAP25. Immunoprecipitation experiments using an anti-FLAG Ab and lysates of PC12 cells transfected with HA-tagged ubiquitin, FLAG-tagged SNAP25, and EGFP-tagged WT CSPα or Ser/Ala mutants showed that CSPα(S34A) and CSPα(S10A/S34A) mutants promoted ubiquitination on FLAG-tagged SNAP25 (Fig. 5*A*). Next, we confirmed the effect of CSPα on expression levels of SNAP25 protein in PC12 cells. There is a significant difference in SNAP25 protein level between WT CSPα and control (Fig. 5*B*), suggesting that CSPα may have a chaperone effect on SNAP25 in PC12 cells. Further, we investigated the effect of CSPα Ser/Ala mutants on the protein level of SNAP25. The SNAP25 protein level decreased when the experiment was conducted with the CSPα(S34A) or CSPα(S10A/S34A) mutants, compared with WT CSPα (Fig. 5*B*). We also investigated the effect of CSPα(S10D/S34D) on SNAP25 protein level, finding that it did not differ from the effect of WT CSPα (Fig. 5*B*). Because a large proportion of CSPα is phosphorylated in PC12 cells, phosphomimetic mutants may not have any additional effect on SNAP25 protein levels compared with WT CSPα. These results suggest that CSPα phosphorylation at Ser10 and Ser34, but predominantly at S34, might play important roles for maintaining the normal conformation of SNAP25 through HSC70/HSP70 chaperone activity.
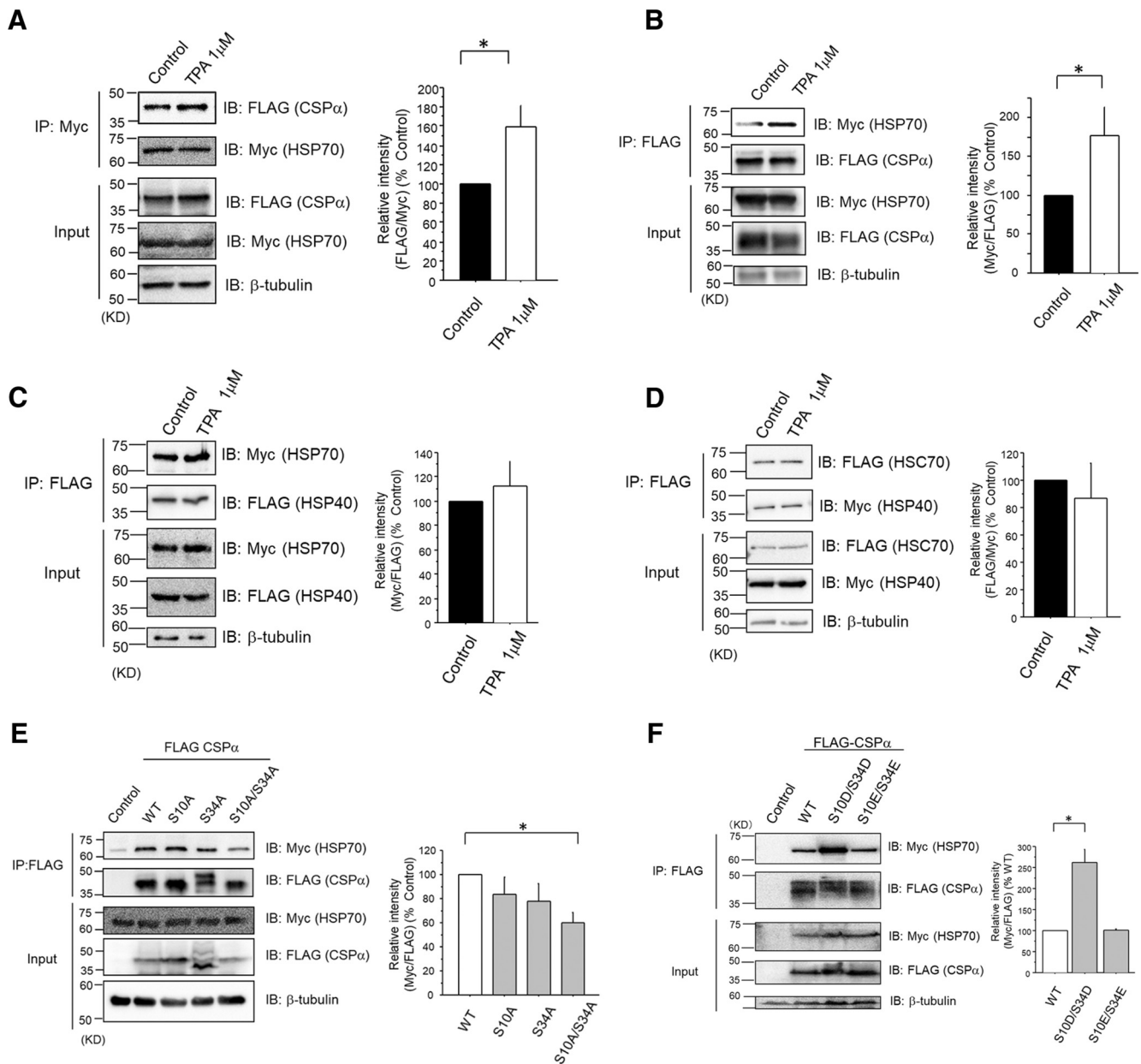
Figure 3. Phosphorylation of CSPα, at Ser10 and Ser34, promotes cell survival. ***A***, Immunoblot for anti-cleaved caspase-3 Ab after treatment with 1 μ$_M$ GFX, or Gö6976, for 72 h was examined in PC12 cells. The right bar graphs represent the cleaved caspase-3 levels with PKC inhibitors, normalized to the control levels, which were set to 100%. The results are expressed as mean ± SEM (n = 4; *p < 0.05, unpaired t test). ***B***, Immunoblot for anti-cleaved caspase-3 was examined with 0, 40, 200, and 1000 n$_M$ Gö6976 for 72 h. The cleaved caspase-3 levels with Gö6976 were normalized to the levels without Gö6976, which were set to 100%, as shown in the right graph (n = 4; *p < 0.05 vs control, 1-way ANOVA with *post hoc* Dunnett's test). The results are expressed as mean ± SEM. ***C***, Immunoblot for anti-cleaved caspase-3 was examined in PC12 cells transfected with control, shRNA for CSPα, and both shRNA for CSPα and CSPα WT with shRNA-resistant sequences. The bar graph represents the quantification of the cleaved caspase-3 levels with shRNA and with shRNA and CSPα WT, normalized to the levels of control, which were set to 100%. The results are expressed as mean ± SEM (n = 9, *p < 0.05 1-way ANOVA with *post hoc* Tukey's test). ***D***, Immunoblot for anti-cleaved caspase-3 was evaluated in PC12 cells transfected with FLAG-tagged CSPα (WT and Ser/Ala mutants). The levels of endogenous CSPα and exogenous CSPα were confirmed. Comparable levels of all ectopically expressed CSPα proteins were confirmed by Western blot analyses. The cleaved caspase-3 levels of CSPα mutants were normalized to the levels of WT, which were set to 100%, as shown in the right bar graph. The results are expressed as mean ± SEM (n = 6, *p < 0.05 vs WT, 1-way ANOVA with *post hoc* Dunnett's test). ***E***, Immunoblot for anti-cleaved caspase-3, evaluated in SHSY5Y cells transfected with FLAG-tagged CSPα (WT and Ser/Ala mutants). The levels of endogenous CSPα and exogenous CSPα were confirmed. Comparable levels of all ectopically expressed CSPα proteins were confirmed by Western blot analyses. The cleaved caspase-3 levels of the CSPα mutants were normalized to the levels of WT, which were set to 100%, as shown in the bar graph. The results are expressed as mean ± SEM (n = 4, *p < 0.05 vs WT, 1-way ANOVA with *post hoc* Dunnett's test). ***F***, Immunoblot for anti-cleaved caspase-3 was evaluated in PC12 cells transfected with FLAG-tagged CSPα (WT, Ser/Glu, and Ser/Asp mutants). The levels of endogenous CSPα and exogenous CSPα were confirmed. Comparable levels of all ectopically expressed CSPα proteins were confirmed by Western blot analyses. The cleaved caspase-3 levels of the CSPα mutants were normalized to the levels of WT, which were set to 100%, as shown in the bar graph. The results are expressed as mean ± SEM (n = 3).

CSPα phosphorylation and SNAP25 protein level decrease in PKCγ KO mice in an age-dependent manner

Finally, we investigated whether these changes in cultured cells are true in mice *in vivo*. To confirm decreased phosphorylation of CSPα in the striatum of PKCγ KO mice, we performed immunoprecipitation experiments with an anti-CSPα Ab, followed by

immunoblotting for an anti-pSer PKC motif Ab. Although phosphorylation levels of CSPα had not significantly decreased in the striata of PKCγ-KO mice at 1 year of age (Fig. 6*A*), we found a reduction in the striata of 2-year-old PKCγ-KO mice, compared with those of WT mice (Fig. 6*B*). These findings were consistent with the results of the phosphoproteome of our previous report
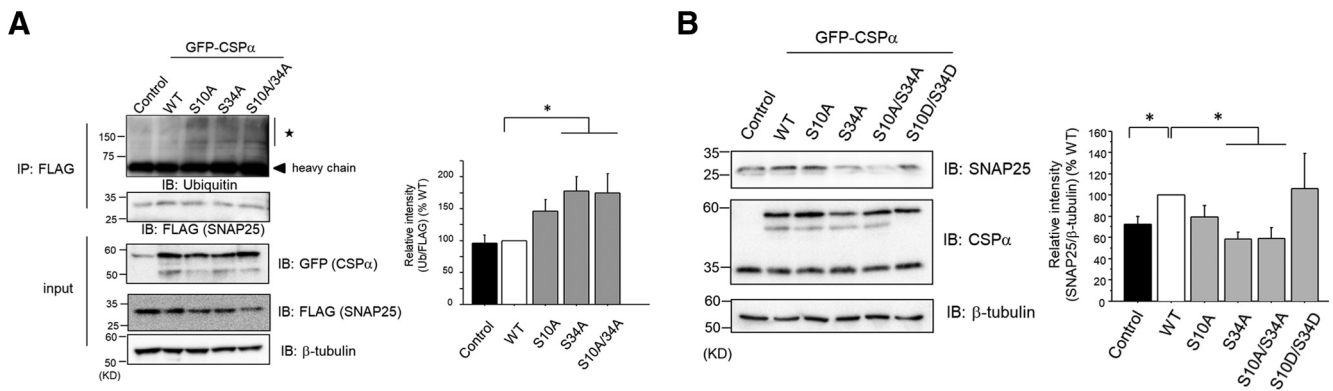
Figure 4. Phosphorylation of CSPα at Ser10 and Ser34 promotes the interaction with HSP70 in PC12 cells. ***A***, Coimmunoprecipitation assay with anti-Myc Ab was performed with COS7 transfected with Myc-tagged HSP70 and FLAG-tagged WT CSPα in the presence or absence of 1 μM TPA. The interaction of Myc-tagged HSP70 and FLAG-tagged WT CSPα was normalized to the level of the control, as shown in the bar graph. The results are expressed as mean ± SEM ($n = 4$, *$p < 0.05$, unpaired t test). ***B***, Coimmunoprecipitation assay with anti-FLAG Ab was performed with COS7, transfected with Myc-tagged HSP70, and FLAG-tagged WT CSPα in the presence or absence of 1 μM TPA. The interaction of Myc-tagged HSP70 and FLAG-tagged WT CSPα was normalized to the level of the control, as shown in the bar graph. The results are expressed as mean ± SEM ($n = 9$, *$p < 0.05$, unpaired t test). ***C***, Coimmunoprecipitation assay with anti-FLAG Ab was performed with COS7, transfected with Myc-tagged HSP70, and FLAG-tagged HSP40 in the presence or absence of 1 μM TPA. The interaction of Myc-tagged HSP70 and FLAG-tagged HSP40 was normalized to the level of the control, as shown in the bar graph. The results are expressed as mean ± SEM ($n = 4$, $p > 0.05$, unpaired t test). ***D***, Coimmunoprecipitation assay with anti-FLAG Ab was performed with COS7, transfected with Myc-tagged HSC70, and FLAG-tagged HSP40 in the presence or absence of 1 μM TPA. The interaction of Myc-tagged HSC70 and FLAG-tagged HSP40 was normalized to the level of the control, as shown in the bar graph. The results are expressed as mean ± SEM ($n = 4$, $p > 0.05$, unpaired t test). ***E***, Coimmunoprecipitation assay with anti-FLAG Ab was performed with COS7, transfected with Myc-tagged HSP70, and FLAG-tagged CSPα (WT and Ser/Ala mutants) was normalized to the level of WT. The results are expressed as mean ± SEM ($n = 5$, *$p < 0.05$ vs WT, 1-way ANOVA with *post hoc* Dunnett's test). ***F***, Coimmunoprecipitation assay with anti-FLAG Ab was performed with COS7, transfected with Myc-tagged HSP70, and FLAG-tagged CSPα (WT, Ser/Asp, and Ser/Glu mutants). The interaction of Myc-tagged HSP70 and FLAG-tagged CSPα (WT, Ser/Asp, and Ser/Glu mutants) was normalized to the level of WT, as shown in the bar graph. The results are expressed as mean ± SEM ($n = 3$, *$p < 0.05$ vs WT, 1-way ANOVA with *post hoc* Dunnett's test).

(Shirafuji et al., 2014). We further evaluated SNAP25 protein levels and ubiquitination for SNAP25 in PKCγ-KO mice. We found that SNAP25 protein levels were not changed in PKCγ-KO mice at 1 year of age (Fig. 6C). However, SNAP25 protein levels declined in the striata of PKCγ-KO mice at the age of 2 years, even

though the protein levels of TH, an indicator of the damage of dopaminergic neurons of the striatum, remained steady (Fig. 6D). In support of our results, previous reports have shown that when a loss of dopaminergic neurons occurs in the SN, the remaining dopamine neurons eventually promote compensatory

Figure 5. Phosphorylation of CSPα at Ser10 and Ser34 increases the ubiquitination/degradation of SNAP25 in PC12 cells. ***A***, Isolated FLAG-tagged SNAP25 by anti-FLAG Ab from PC12 cells, transfected with GFP-tagged CSPα (WT and Ser/Ala mutants) and FLAG-tagged SNAP25 and HA-tagged ubiquitin, was immunoblotted by anti-ubiquitin Ab. The ubiquitin levels of FLAG-tagged SNAP25 from PC12 cells transfected with GFP-tagged CSPα (WT and Ser/Ala mutants) were normalized with respect to WT, as shown in the bar graph. The results are expressed as mean ± SEM (n = 5, *$p < 0.05$ vs WT, 1-way ANOVA with *post hoc* Dunnett's test). The star indicates the ubiquitinated FLAG-tagged SNAP25. ***B***, Endogenous SNAP25 protein levels were measured in PC12 cells transfected with GFP-tagged CSPα (WT, Ser/Ala mutants, and Ser/Asp mutant) by using immunoblot for anti-SNAP25 Ab. SNAP25 protein levels were normalized with respect to WT, as shown in the bar graph. The results are expressed as mean ± SEM (Control, n = 12; WT, n = 13; S10A, n = 7; S34A, n = 7; S10A/S34A, n = 13; S10D/S34D, n = 8; *$p < 0.05$ vs WT, 1-way ANOVA with *post hoc* Games–Howell's test).

axonal sprouting and new dopaminergic synapse formation (Finkelstein et al., 2000; Arkadir et al., 2014). These findings suggest that PKCγ, through CSPα phosphorylation *in vivo*, protects dopaminergic neurons by modulating the CSPα–HSC70/HSP70–SNAP25 axis.

Discussion

In the present study, we discovered a novel phosphorylation site of CSPα, Ser34, in the helix II of the J domain, for phosphorylation by PKCγ, in addition to the previously reported site, Ser10 (Evans et al., 2001, 2006). We also demonstrated that double phosphorylation of CSPα at Ser10 and Ser34 by PKCγ promotes the interaction between CSPα and HSC70/HSP70, which further induces HSC70/HSP70 chaperone activity for SNAP25 and eventually supports neuronal cell survival. In the striata of 2-year-old PKCγ-KO mice, decreased phosphorylation levels of CSPα and decreased SNAP25 protein levels were observed. Thus, we propose the PKCγ–CSPα–HSC70/HSP70–SNAP25 signaling axis, in which the Ca^{2+}-dependent PKC isoform PKCγ protects the presynaptic terminal through CSPα phosphorylation at Ser10 and Ser34.

### Phosphorylation sites of CSPα, targeted by PKCγ
In our previous study, we demonstrated that Ser10 of CSPα is a potent PKCγ substrate for phosphorylation in the mice striatum (Shirafuji et al., 2014). CSPα has been reported to be phosphorylated at Ser10 in rat brains (Evans and Morgan, 2005). Earlier reports (Evans et al., 2001, 2006) also demonstrated that PKA and protein kinase B/Akt phosphorylate CSPα at Ser10, which was previously the only reported phosphorylation site on CSPα. Phosphorylation of CSPα at Ser10 has been reported to modulate the binding affinity of CSPα for key exocytotic proteins, including syntaxin, synaptotagmin (Evans and Morgan, 2002; Evans et al., 2006), and the 14-3-3 protein (Prescott et al., 2008). These findings suggested that phosphorylation of CSPα at Ser10 may be important for interaction with other proteins and associated with various cell functions. In contrast, CSPα Ser10 phosphorylation has been reported to have no function involving interaction with HSP70 (Evans et al., 2001; Boal et al., 2011). In the present study, we demonstrated for the first time that human CSPα Ser34 in the helix II of the J domain is a cPKC phosphorylation site. As HPD

motif and helix II in the J domain are important for interaction with HSC70/HSP70 (Tsai and Douglas, 1996; Greene et al., 1998), CSPα Ser34 phosphorylation is assumed to promote interaction with the HSC70/HSP70 complex. We propose here that CSPα phosphorylation at both Ser10 and Ser34 may have important functions for interaction with HSC70/HSP70. We suggest two reasons: (1) within the CSPα–HSC70/HSP70–SGT complex, only CSPα was phosphorylated upon the activation of cPKC (Fig. 1 *B*,*C*), and (2) the CSPα(S10A/S34A) mutant showed impaired binding between HSP70 and CSPα (Fig. 4*E*). The reason why the double mutant exhibits a stronger effect than CSPα(S34A), when the other single mutant, CSPα(S10A), displays no effect, remains unclear. However, the possible mechanism may be that CSPα Ser10 phosphorylation may help the interaction with HSC70/HSP70 by Ser34 phosphorylation through a conformational change because, as has been reported, CSPα Ser10 phosphorylation triggers a major conformational change (Patel et al., 2016). In line with this speculation, Ser34 phosphorylation is necessary for Ser10 phosphorylation by PKC because the CSPα(S34A) mutant was not phosphorylated by TPA, a PKC stimulator (Fig. 2*B*).

Comparison of CSPα phosphorylation sites
CSPα Ser10 is conserved through the species, from *Drosophila melanogaster* to *Homo sapiens*. Ser34 is also relatively conserved within fish (*Danio rerio*), and humans, although not in *D. melanogaster* (Thr) and *Xenopus laevis* (Cys; Fig. 7). As Cys has a negative charge like the phosphoryl group, CSP of *X. laevis* may function the same as the CSPs of other species with Ser. As the CSPα(S10D/S34D) mutant, but not CSPα(S10E/S34E) mutant, interacted with HSP70 more strongly than WT CSPα (Fig. 4*F*), phosphorylated Ser, not Thr, may be crucial for the interaction of CSPα with HSP70. CSPα belongs to the HSP40 type-3 (also called DNAJC5) subtype, and is specifically expressed on the synaptic vesicles in the presynaptic terminal in neurons. CSPα Ser34 in the helix II of J domain is located 9 aa upstream from the HPD motif (Szyperski et al., 1994; Hill et al., 1995), which is crucial for interaction with HSC70/HSP70. The amino acid corresponding to Ser34 of CSPα is Ala in almost all members of the human HSP40/DNAJ families (Walsh et al., 2004), and it is converted into Ser residue only in human DNAJC5 (CSPα), DNAJC22, and DNAJC28. Moreover, CSPα has been reported to be modulated,
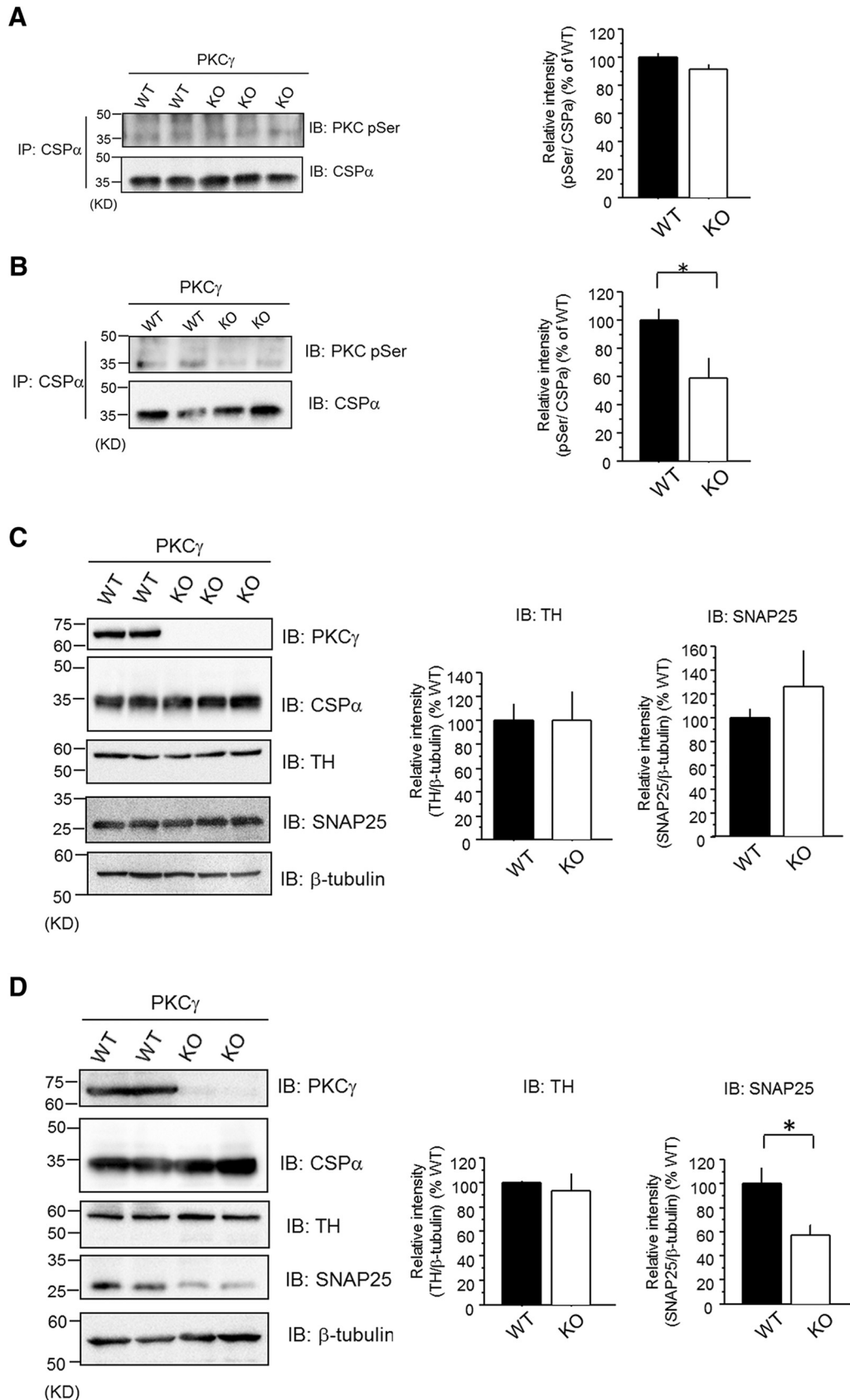
Figure 6.   Decreased levels of CSPα phosphorylation and SNAP25 protein levels in the PKCγ-KO mouse striatum. *A*, Isolated CSPα by anti-CSPα Ab from the striatum of 1-year-old PKCγ-KO and WT mice was immunoblotted with anti-pSer PKC motif Ab. The right bar graph represents the quantification of pSer levels normalized to respect to WT. The results are expressed as mean ± SEM (WT, *n* = 4; KO, *n* = 5; not significant, unpaired *t* test). *B*, Isolated CSPα by anti-CSPα Ab from the striatum of 2-year-old PKCγ-KO and WT mice was immunoblotted with anti-pSer PKC motif Ab. The right bar graph represents the quantification of pSer levels normalized to respect to WT. The results are expressed as mean ± SEM (WT, *n* = 5; (*Figure legend continues.*)

	10	34
H. Sapiens	RQRSL**S**TSGES	DDIKK**S**YRKLA
M. Musculus	RQRSL**S**TSGES	DDIKK**S**YRKLA
R. Norvegicus	RQRSL**S**TSGES	DDIKK**S**YRKLA
G. Gallus	RQRSL**S**TSGES	DDIKK**S**YRKLA
X. Laevis	RQRSL**S**TSGES	DDIKK**C**YRKLA
D. Rerio	RQRSL**S**TSGES	DDIKK**S**YRKLA
D. melanogaster	DKRKL**S**TSGDS	DDIKK**T**YRKLA

Figure 7. Schematic comparisons of CSPα Ser10 and Ser34 through evolution. CSPα Ser10 is evolutionarily conserved in all species listed. Notably, CSPα Ser34 is relatively conserved between *Danio rerio* and *Homo sapiens*, although not in the *D. melanogaster* and *X. laevis* species.

through palmitoylation, to tether to membranes on the synaptic vesicles (Greaves et al., 2008). Because PKC easily phosphorylates membrane-bound proteins (Shirai et al., 1998), CSPα may become a good substrate of PKC through palmitoylation. As shown in Figure 4, TPA promoted the interaction between CSPα and HSP70, but not between HSP40 and HSP70 (Fig. 4A–D). Collectively, CSPα with Ser34, which is potentially phosphorylated by PKCγ, may be, compared with other HSP40 cochaperone families, more specifically evolved for serving HSC70/HSP70 chaperone activity in presynaptic terminals.

Downstream cascade of phosphorylated CSPα

How can CSPα regulate neuronal cell survival through phosphorylation? Previous reports identified many targets of CSPα (Leveque et al., 1998; Wu et al., 1999; Magga et al., 2000; Evans and Morgan, 2002; Sakisaka et al., 2002; Boal et al., 2004, 2011; Chandra et al., 2005; Sharma et al., 2011; Shirasaki et al., 2012; Zhang et al., 2012). Among them, SNAP25 is a critical target of the CSPα–HSC70/HSP70–SGT complex (Sharma et al., 2011, 2012) for the maintenance of the presynaptic terminal. In our 2-year-old PKCγ-KO mice, levels of CSPα phosphorylation and SNAP25 protein decreased significantly (Fig. 6B,D). Indeed, a previous report demonstrated an elevated ubiquitination level in dopaminergic and serotonergic neurons of PKCγ-KO rats (Al-Kushi, 2007). In line with our results obtained from PKCγ-KO mice, dysfunctional SNAP25 with abnormal conformation is ubiquitinated and degraded by the proteasome in a synaptic activity-dependent manner in CSPα-deficient mice, which exhibit presynaptic degeneration and neurodegeneration (Sharma et al., 2011, 2012). The number of neurons in the SN was lower at 13–14 months than at 10–12 months in PKCγ-KO rats (Payne et al., 2000). As shown in Figure 6, the SNAP25 protein level was lower at 24 months compared with the level at 12 months. These findings suggest that the decline in SNAP25 may be correlated with decreased numbers of SN neurons. Collectively, CSPα phosphorylation by PKCγ may maintain the normal conformation of

SNAP25 and protect the synaptic terminal by promoting the HSC70/HSP70 chaperone activity.

PKCγ–CSPα–HSC70/HSP70–SNAP25 axis protects the presynaptic terminal

In neurodegenerative diseases, there is an early degeneration of presynaptic terminals before the loss of neuronal somata (Wishart et al., 2006). CSPα is a synaptic protein thought capable of directly modulating the stability and/or degeneration of the presynaptic terminal (Gillingwater and Wishart, 2013). It has also been shown that mice lacking CSPα are susceptible to a synaptic degeneration phenotype (Fernández-Chacón et al., 2004). Indeed, reduced CSPα expression contributes to the initial stages of synaptic degeneration in patients with Alzheimer's disease (AD; Tiwari et al., 2015). Thus, CSPα dysfunction, such as decreased phosphorylation, may be related to presynaptic degeneration observed in the early stage of neurodegenerative diseases. In line with this speculation, apoptosis increased and SNAP25 protein level decreased in a CSPα phosphorylation-null mutant in PC12 cells (Figs. 3D, 5B). Improving the PKCγ–CSPα–HSC70/HSP70–SNAP25 pathway may prevent neurodegenerative diseases by facilitating the HSC70/HSP70 chaperone function.

PKCγ may protect the presynaptic terminal in association with Ca²⁺-triggered exocytosis

The synaptic vesicle cycle (exocytosis and endocytosis) occurs during neuronal activity. Ca^{2+}-dependent PKCs are also activated by neuronal activity in the rat hippocampus (Brager and Thompson, 2003). Many studies have shown that Ca^{2+}-stimulated exocytosis is controlled by PKC through the phosphorylation of components of the exocytotic machinery, such as SNAP25, Munc18, and βPIX (Iwasaki et al., 2000; Barclay et al., 2003; Shirafuji et al., 2014). It has been suggested that neuronal activity and exocytosis/endocytosis is involved in neurodegeneration (Cirrito et al., 2005; García-Junco-Clemente et al., 2010; Koch et al., 2011). Thus, cPKC may be related to neurodegeneration in association with exocytosis/endocytosis. In CSPα-deficient mice, presynaptic degeneration occurs in a neuronal activity-dependent manner (Sharma et al., 2011). This CSPα-dependent protection for the presynaptic terminal might be modulated by PKCγ, downstream of Ca^{2+} influx. Together, cPKC, including PKCγ, may play important roles for maintaining homeostasis in the presynaptic terminal, which is the damaged site in neurodegenerative diseases, occurring at an early stage through CSPα phosphorylation, in association with Ca^{2+}-stimulated exocytosis, or neuronal activity.

Dysfunction of PKC activation in aging

Dysfunction of PKC activity has been reported in aging. During aging, lipid environment alteration and changes in protein–protein interactions may impair the mechanisms of PKC activation (Battaini and Pascale, 2005). In rodents, despite steady PKC isoform protein levels, the activation/translocation processes of the PKCs are impaired in aged brains (Friedman and Wang, 1989; Battaini et al., 1995; Pascale et al., 1996). Human studies have shown that dysfunction of PKC activation is caused by lower expression levels of its adaptor protein, receptor of activated protein C kinase 1 (RACK1), in pathologically aged brain, such as in AD (Battaini et al., 1999). From our results obtained in PKCγ-KO mice, decreased levels of CSPα phosphorylation and SNAP25 protein in the striatum may also occur in the aging human brain. Thus, in the primary process of neurodegeneration, the dysfunction of the

←

(*Figure legend continued.*) KO, $n = 6$; *$p < 0.05$, unpaired t test. **C**, The protein level of SNAP25 and TH in the striatum of 1-year-old mice was examined by immunoblot with anti-SNAP25 Ab and anti-TH Ab. The right bar graphs represent the quantification of TH and SNAP25 protein levels normalized with respect to WT, respectively. The results are expressed as mean ± SEM (TH: WT, $n = 4$; KO, $n = 5$, not significant, unpaired t test; SNAP25: WT, $n = 4$; KO, $n = 5$, not significant, unpaired t test). **D**, The protein level of SNAP25 and TH in the striatum of 2-year-old mice was measured by immunoblot with anti-SNAP25 Ab and anti-TH Ab. The right bar graphs on the right represent the quantification of TH and SNAP25 protein levels normalized with respect to WT. The results are expressed as mean ± SEM (TH: WT, $n = 3$; KO, $n = 4$, not significant, unpaired t test; SNAP25: WT, $n = 5$; KO, $n = 6$, *$p < 0.05$, unpaired t test).

PKCγ–CSPα–HSC70/HSP70–SNAP25 axis caused by aging may promote the development of the neurodegeneration.

In conclusion, PKCγ may promote HSC70/HSP70 chaperone activity through CSPα phosphorylation at both Ser10 and Ser34 in the presynaptic terminal of dopaminergic neurons. Phosphorylation modulation of CSPα by PKC may be a potential therapeutic target for the treatment of early stages of neurodegenerative diseases, especially PD.

References

Al-Kushi AG (2007) Pathological change in mesostriatal neurons in a PKC-gamma mutant rat. PhD thesis. University of Glasgow.

Arkadir D, Bergman H, Fahn S (2014) Redundant dopaminergic activity may enable compensatory axonal sprouting in Parkinson disease. Neurology 82:1093–1098. CrossRef Medline

Barclay JW, Craig TJ, Fisher RJ, Ciufo LF, Evans GJ, Morgan A, Burgoyne RD (2003) Phosphorylation of Munc18 by protein kinase C regulates the kinetics of exocytosis. J Biol Chem 278:10538–10545. CrossRef Medline

Battaini F, Pascale A (2005) Protein kinase C signal transduction regulation in physiological and pathological aging. Ann N Y Acad Sci 1057:177–192. CrossRef Medline

Battaini F, Elkabes S, Bergamaschi S, Ladisa V, Lucchi L, De Graan PN, Schuurman T, Wetsel WC, Trabucchi M, Govoni S (1995) Protein kinase C activity, translocation, and conventional isoforms in aging rat brain. Neurobiol Aging 16:137–148. CrossRef Medline

Battaini F, Pascale A, Lucchi L, Pasinetti GM, Govoni S (1999) Protein kinase C anchoring deficit in postmortem brains of Alzheimer's disease patients. Exp Neurol 159:559–564. CrossRef Medline

Boal F, Zhang H, Tessier C, Scotti P, Lang J (2004) The variable C-terminus of cysteine string proteins modulates exocytosis and protein–protein interactions. Biochemistry 43:16212–16223. CrossRef Medline

Boal F, Laguerre M, Milochau A, Lang J, Scotti PA (2011) A charged prominence in the linker domain of the cysteine-string protein Cspα mediates its regulated interaction with the calcium sensor synaptotagmin 9 during exocytosis. FASEB J 25:132–143. CrossRef Medline

Brager DH, Thompson SM (2003) Activity-dependent release of adenosine contributes to short-term depression at CA3-CA1 synapses in rat hippocampus. J Neurophysiol 89:22–26. CrossRef Medline

Braun JE, Wilbanks SM, Scheller RH (1996) The cysteine string secretory vesicle protein activates Hsc70 ATPase. J Biol Chem 271:25989–25993. CrossRef Medline

Burgoyne RD, Morgan A (2015) Cysteine string protein (CSP) and its role in preventing neurodegeneration. Seminars in cell and developmental biology 40:153–159. CrossRef Medline

Chamberlain LH, Burgoyne RD (1997) Activation of the ATPase activity of heat-shock proteins Hsc70/Hsp70 by cysteine-string protein. Biochem J 322:853–858. CrossRef Medline

Chamberlain LH, Burgoyne RD (2000) Cysteine-string protein: the chaperone at the synapse. J Neurochem 74:1781–1789. Medline

Chandra S, Gallardo G, Fernández-Chacón R, Schlüter OM, Südhof TC (2005) Alpha-synuclein cooperates with CSPalpha in preventing neurodegeneration. Cell 123:383–396. CrossRef Medline

Cheetham ME, Caplan AJ (1998) Structure, function and evolution of DnaJ: conservation and adaptation of chaperone function. Cell Stress Chaperones 3:28–36. CrossRef Medline

Cirrito JR, Yamada KA, Finn MB, Sloviter RS, Bales KR, May PC, Schoepp DD, Paul SM, Mennerick S, Holtzman DM (2005) Synaptic activity regulates interstitial fluid amyloid-beta levels in vivo. Neuron 48:913–922. CrossRef Medline

Ding YQ, Xiang CX, Chen ZF (2005) Generation and characterization of the PKC gamma-Cre mouse line. Genesis 43:28–33. CrossRef Medline

Evans GJ, Morgan A (2002) Phosphorylation-dependent interaction of the synaptic vesicle proteins cysteine string protein and synaptotagmin I. Biochem J 364:343–347. CrossRef Medline

Evans GJ, Morgan A (2005) Phosphorylation of cysteine string protein in the brain: developmental, regional and synaptic specificity. Eur J Neurosci 21:2671–2680. CrossRef Medline

Evans GJ, Wilkinson MC, Graham ME, Turner KM, Chamberlain LH, Burgoyne RD, Morgan A (2001) Phosphorylation of cysteine string protein by protein kinase A. Implications for the modulation of exocytosis. J Biol Chem 276:47877–47885. CrossRef Medline

Evans GJ, Barclay JW, Prescott GR, Jo SR, Burgoyne RD, Birnbaum MJ, Morgan A (2006) Protein kinase B/Akt is a novel cysteine string protein kinase that regulates exocytosis release kinetics and quantal size. J Biol Chem 281:1564–1572. CrossRef Medline

Fang S, Crews AL, Chen W, Park J, Yin Q, Ren XR, Adler KB (2013) MARCKS and HSP70 interactions regulate mucin secretion by human airway epithelial cells in vitro. Am J Physiol Lung Cell Mol Physiol 304: L511–L518. CrossRef Medline

Fernández-Chacón R, Wölfel M, Nishimune H, Tabares L, Schmitz F, Castellano-Muñoz M, Rosenmund C, Montesinos ML, Sanes JR, Schneggenburger R, Südhof TC (2004) The synaptic vesicle protein CSP alpha prevents presynaptic degeneration. Neuron 42:237–251. CrossRef Medline

Finkelstein DI, Stanic D, Parish CL, Tomas D, Dickson K, Horne MK (2000) Axonal sprouting following lesions of the rat substantia nigra. Neuroscience 97:99–112. CrossRef Medline

Friedman E, Wang HY (1989) Effect of age on brain cortical protein kinase C and its mediation of 5-hydroxytryptamine release. J Neurochem 52: 187–192. CrossRef Medline

García-Junco-Clemente P, Cantero G, Gómez-Sánchez L, Linares-Clemente P, Martínez-López JA, Luján R, Fernández-Chacón R (2010) Cysteine string protein-α prevents activity-dependent degeneration in GABAergic synapses. J Neurosci 30:7377–7391. CrossRef Medline

Gillingwater TH, Wishart TM (2013) Mechanisms underlying synaptic vulnerability and degeneration in neurodegenerative disease. Neuropathol Appl Neurobiol 39:320–334. CrossRef Medline

Greaves J, Salaun C, Fukata Y, Fukata M, Chamberlain LH (2008) Palmitoylation and membrane interactions of the neuroprotective chaperone cysteine-string protein. J Biol Chem 283:25014–25026. CrossRef Medline

Greene MK, Maskos K, Landry SJ (1998) Role of the J-domain in the cooperation of Hsp40 with Hsp70. Proc Natl Acad Sci U S A 95:6108–6113. CrossRef Medline

Hill RB, Flanagan JM, Prestegard JH (1995) 1H and 15N magnetic resonance assignments, secondary structure, and tertiary fold of Escherichia coli DnaJ(1–78). Biochemistry 34:5587–5596. CrossRef Medline

Iwasaki S, Kataoka M, Sekiguchi M, Shimazaki Y, Sato K, Takahashi M (2000) Two distinct mechanisms underlie the stimulation of neurotransmitter release by phorbol esters in clonal rat pheochromocytoma PC12 cells. J Biochem 128:407–414. CrossRef Medline

Kashyap SS, Johnson JR, McCue HV, Chen X, Edmonds MJ, Ayala M, Graham ME, Jenn RC, Barclay JW, Burgoyne RD, Morgan A (2014) Caenorhabditis elegans dnj-14, the orthologue of the DNAJC5 gene mutated in adult onset neuronal ceroid lipofuscinosis, provides a new platform for neuroprotective drug screening and identifies a SIR-2.1-independent action of resveratrol. Hum Mol Genet 23:5916–5927. CrossRef Medline

Koch P, Breuer P, Peitz M, Jungverdorben J, Kesavan J, Poppe D, Doerr J, Ladewig J, Mertens J, Tüting T, Hoffmann P, Klockgether T, Evert BO, Wüllner U, Brüstle O (2011) Excitation-induced ataxin-3 aggregation in neurons from patients with Machado-Joseph disease. Nature 480:543–546. Medline

Kohan SA, Pescatori M, Brecha NC, Mastrogiacomo A, Umbach JA, Gundersen CB (1995) Cysteine string protein immunoreactivity in the nervous system and adrenal gland of rat. J Neurosci 15:6230–6238. Medline

Leveque C, Pupier S, Marqueze B, Geslin L, Kataoka M, Takahashi M, De Waard M, Seagar M (1998) Interaction of cysteine string proteins with the alpha1A subunit of the P/Q-type calcium channel. J Biol Chem 273: 13488–13492. CrossRef Medline

Magga JM, Jarvis SE, Arnot MI, Zamponi GW, Braun JE (2000) Cysteine string protein regulates G-protein modulation of N-type calcium channels. Neuron 28:195–204. CrossRef Medline

Murray D, Honig B (2002) Electrostatic control of the membrane targeting of C2 domains. Mol Cell 9:145–154. CrossRef Medline

Nagano Y, Yamashita H, Takahashi T, Kishida S, Nakamura T, Iseki E, Hattori N, Mizuno Y, Kikuchi A, Matsumoto M (2003) Siah-1 facilitates ubiquitination and degradation of synphilin-1. J Biol Chem 278:51504–51514. CrossRef Medline

Nishizuka Y (1992) Intracellular signaling by hydrolysis of phospholipids and activation of protein kinase C. Science 258:607–614. CrossRef Medline

Ohtsuka K (1993) Cloning of a cDNA for heat-shock protein hsp40, a human homologue of bacterial DnaJ. Biochem Biophys Res Commun 197: 235–240. CrossRef Medline

Ota T, Suzuki Y, Nishikawa T, Otsuki T, Sugiyama T, Irie R, Wakamatsu A, Hayashi K, Sato H, Nagai K, Kimura K, Makita H, Sekine M, Obayashi M, Nishi T, Shibahara T, Tanaka T, Ishii S, Yamamoto J, Saito K, et al. (2004) Complete sequencing and characterization of 21,243 full-length human cDNAs. Nat Genet 36:40 – 45. CrossRef Medline

Pascale A, Fortino I, Govoni S, Trabucchi M, Wetsel WC, Battaini F (1996) Functional impairment in protein kinase C by RACK1 (receptor for activated C kinase 1) deficiency in aged rat brain cortex. J Neurochem 67: 2471–2477. Medline

Patel P, Prescott GR, Burgoyne RD, Lian LY, Morgan A (2016) Phosphorylation of cysteine string protein triggers a major conformational switch. Structure 24:1380 –1386. CrossRef Medline

Payne AP, Campbell JM, Russell D, Favor G, Sutcliffe RG, Bennett NK, Davies RW, Stone TW (2000) The AS/AGU rat: a spontaneous model of disruption and degeneration in the nigrostriatal dopaminergic system. J Anat 196:629 – 633. CrossRef Medline

Prescott GR, Jenkins RE, Walsh CM, Morgan A (2008) Phosphorylation of cysteine string protein on Serine 10 triggers 14-3-3 protein binding. Biochem Biophys Res Commun 377:809 – 814. CrossRef Medline

Qiu XB, Shao YM, Miao S, Wang L (2006) The diversity of the DnaJ/Hsp40 family, the crucial partners for Hsp70 chaperones. Cell Mol Life Sci 63: 2560 –2570. CrossRef Medline

Ruvolo PP, Deng X, Carr BK, May WS (1998) A functional role for mitochondrial protein kinase Calpha in Bcl2 phosphorylation and suppression of apoptosis. J Biol Chem 273:25436 –25442. CrossRef Medline

Saito N, Shirai Y (2002) Protein kinase C gamma (PKC gamma): function of neuron specific isotype. J Biochem 132:683– 687. CrossRef Medline

Sakisaka T, Meerlo T, Matteson J, Plutner H, Balch WE (2002) Rab-alphaGDI activity is regulated by a Hsp90 chaperone complex. EMBO J 21:6125– 6135. CrossRef Medline

Sharma M, Burré J, SüdhofTC (2011) CSPalpha promotes SNARE-complex assembly by chaperoning SNAP-25 during synaptic activity. Nat Cell Biol 13:30 –39. CrossRef Medline

Sharma M, Burré J, Bronk P, Zhang Y, Xu W, Südhof TC (2012) CSPalpha knockout causes neurodegeneration by impairing SNAP-25 function. The EMBO J 31:829 – 841. CrossRef Medline

Shirafuji T, Ueyama T, Yoshino K, Takahashi H, Adachi N, Ago Y, Koda K, Nashida T, Hiramatsu N, Matsuda T, Toda T, Sakai N, Saito N (2014) The role of Pak-interacting exchange factor-β phosphorylation at serines 340 and 583 by PKCγ in dopamine release. J Neurosci 34:9268 –9280. CrossRef Medline

Shirafuji T, Ueyama T, Tanaka S, Hide I, Saito N, Sakai N (2017) Validation of anti-CSPalpha, SNAP25, tyrosine hydroxylase, ubiquitin, cleaved caspase3, adn pSer PKC motif antibodies for utilization in Western blotting. Acta Histochem Cytochem, in press.

Shirai Y, Sakai N, Saito N (1998) Subspecies-specific targeting mechanism of protein kinase C. Jpn J Pharmacol 78:411– 417. CrossRef Medline

Shirasaki DI, Greiner ER, Al-Ramahi I, Gray M, Boontheung P, Geschwind DH, Botas J, Coppola G, Horvath S, Loo JA, Yang XW (2012) Network organization of the huntingtin proteomic interactome in mammalian brain. Neuron 75:41–57. CrossRef Medline

Szyperski T, Pellecchia M, Wall D, Georgopoulos C, Wüthrich K (1994) NMR structure determination of the *Escherichia coli* DnaJ molecular chaperone: secondary structure and backbone fold of the N-terminal region (residues 2–108) containing the highly conserved J domain. Proc Natl Acad Sci U S A 91:11343–11347. CrossRef Medline

Tiwari SS, d'Orange M, Troakes C, Shurovi BN, Engmann O, Noble W, HortobágyiT, Giese KP (2015) Evidence that the presynaptic vesicle protein CSPalpha is a key player in synaptic degeneration and protection in Alzheimer's disease. Mol Brain 8:6. CrossRef Medline

Tobaben S, Thakur P, Fernández-Chacón R, Südhof TC, Rettig J, Stahl B (2001) A trimeric protein complex functions as a synaptic chaperone machine. Neuron 31:987–999. CrossRef Medline

Tsai J, Douglas MG (1996) A conserved HPD sequence of the J-domain is necessary for YDJ1 stimulation of Hsp70 ATPase activity at a site distinct from substrate binding. J Biol Chem 271:9347–9354. CrossRef Medline

Ueyama T, Tatsuno T, Kawasaki T, Tsujibe S, Shirai Y, Sumimoto H, Leto TL, Saito N (2007) A regulated adaptor function of p40phox: distinct p67phox membrane targeting by p40phox and by p47phox. Mol Biol Cell 18:441– 454. CrossRef Medline

Walsh P, Bursać D, Law YC, Cyr D, Lithgow T (2004) The J-protein family: modulating protein assembly, disassembly and translocation. EMBO Rep 5:567–571. CrossRef Medline

Whelan RD, Parker PJ (1998) Loss of protein kinase C function induces an apoptotic response. Oncogene 16:1939–1944. CrossRef Medline

Wishart TM, Parson SH, Gillingwater TH (2006) Synaptic vulnerability in neurodegenerative disease. J Neuropathol Exp Neurol 65:733–739. CrossRef Medline

Wu MN, Fergestad T, Lloyd TE, He Y, Broadie K, Bellen HJ (1999) Syntaxin 1A interacts with multiple exocytic proteins to regulate neurotransmitter release *in vivo*. Neuron 23:593– 605. CrossRef Medline

Yochem J, Uchida H, Sunshine M, Saito H, Georgopoulos CP, Feiss M (1978) Genetic analysis of two genes, *dnaJ* and *dnaK*, necessary for *Escherichia coli* and bacteriophage lambda DNA replication. Mol Gen Genet 164:9 –14. CrossRef Medline

Zhang YQ, Henderson MX, Colangelo CM, Ginsberg SD, Bruce C, Wu T, Chandra SS (2012) Identification of CSPalpha clients reveals a role in dynamin 1 regulation. Neuron 74:136 –150. CrossRef Medline

Zinsmaier KE, Eberle KK, Buchner E, Walter N, Benzer S (1994) Paralysis and early death in cysteine string protein mutants of *Drosophila*. Science 263:977–980. CrossRef Medline